

# <sup>111</sup>In-DTPA Cisternography with SPECT/CT for the Evaluation of Normal Pressure Hydrocephalus

Daniel P. Thut<sup>1</sup>, Alena Kreychman<sup>1</sup>, and J. Antonio Obando<sup>1,2</sup>

<sup>1</sup>Division of Nuclear Medicine, Department of Diagnostic Radiology, Yale School of Medicine, New Haven, Connecticut; and

<sup>2</sup>Department of Radiology, Veterans Administration CT Healthcare System, West Haven, Connecticut

Although new MR imaging techniques can provide high-resolution information on CSF dynamics and are not associated with ionizing radiation, SPECT/CT cisternography is a valuable alternative for those with contraindications to MR imaging. SPECT/CT cisternography combines functional and anatomic imaging to provide accurate and detailed information on CSF distribution to be used in conjunction with clinical findings for the diagnosis and evaluation of NPH, as illustrated in this case report.

**Key Words:** cisternography; SPECT/CT; normal pressure hydrocephalus; CSF dynamics

**J Nucl Med Technol 2014; 42:1–5**

DOI: 10.2967/jnmt.113.128041

Normal-pressure hydrocephalus (NPH) is a form of communicating hydrocephalus that affects approximately 3% of elderly patients and up to 14% of patients living in extended-care facilities, with an incidence ranging from 2 million to 20 million per year (1,2). The classic, yet non-specific, clinical triad includes progressive dementia, ataxia, and urinary incontinence. Usually these findings, together with normal cerebrospinal fluid (CSF) pressures and radiographic evidence of ventriculomegaly, are required to make the diagnosis.

## CASE REPORT

A 68-y-old man with a history of being in a motor vehicle accident presented with gait disturbance, urinary incontinence, and progressive cognitive decline. Anatomic imaging, including CT and MR imaging, demonstrated dilated ventricles out of proportion to sulcal prominence. NPH was suspected, and the patient underwent <sup>111</sup>In-diethylenetriaminepentaacetic acid (DTPA) cisternography with hybrid SPECT/CT.

Understanding the normal physiology of CSF dynamics is imperative for image interpretation. CSF is produced and secreted primarily by the ventricular choroid plexus and to a lesser extent in other extraventricular sites. Approximately 400–500 mL of CSF are created per day, with a total CSF volume of 120–150 mL, of which only about 40 mL remains in the ventricular system (3). Under normal physiologic conditions, the CSF drains from the lateral ventricles through the foramen of Monro and into the third ventricle. From there, it passes through the cerebral aqueduct of Sylvius and into the fourth ventricle. CSF leaves the ventricular system through the foramen of Magendie and the 2 lateral foramina of Luschka into the subarachnoid space surrounding the brain and spinal cord, as well as the cisterns. Finally, it is absorbed through the pacchionian granulations of the pia arachnoid villi into the superior sagittal sinus. The pathophysiologic basis of NPH is an obstruction in the subarachnoid space that prevents absorption of CSF (4,5). A variety of causes can lead to this extraventricular CSF obstruction. Some common etiologies include prior subarachnoid hemorrhage, chronic subdural hematoma, leptomeningitis, and meningeal carcinomatosis (6).

In our study, we used 18.5 MBq (0.5 mCi) of <sup>111</sup>In-DTPA injected intrathecally into the subarachnoid space via lumbar puncture. <sup>111</sup>In has a relatively long half-life (67 h) and reasonable imaging characteristics. After the injection, an initial image of the site usually confirms the correct location by visualizing the cephalad migration of radiotracer up the spinal canal (Fig. 1). No excessive renal activity should be noted on these early images. Planar views in multiple projections are typically acquired at 2, 4, 24, and 48 h. In a study with normal findings, the radiotracer should reach the basal cisterns within the first hour, the Sylvian fissure by 2–6 h, the cerebral convexities by 12 h, and the arachnoid villi in the sagittal sinus by 24 h (7).

At 24 h, SPECT/CT axial slices through the brain and cervical spine of our patient were obtained and reconstructed into coronal and sagittal planes (Precedence 16-slice CT scanner [Philips]). SPECT was performed using medium-energy general-purpose collimators, a 128 × 128 matrix, 35 s/stop, a step-and-shoot noncircular orbit, ordered-subsets expectation maximization with 3 iterations

Received Jul. 18, 2013; revision accepted Oct. 2, 2013.  
For correspondence or reprints contact: Daniel P. Thut, 175 S. End Rd., E-29, East Haven, CT 06512.  
E-mail: daniel.thut@yale.edu  
Published online ■■■■■■■■■■.  
COPYRIGHT © 2014 by the Society of Nuclear Medicine and Molecular Imaging, Inc.

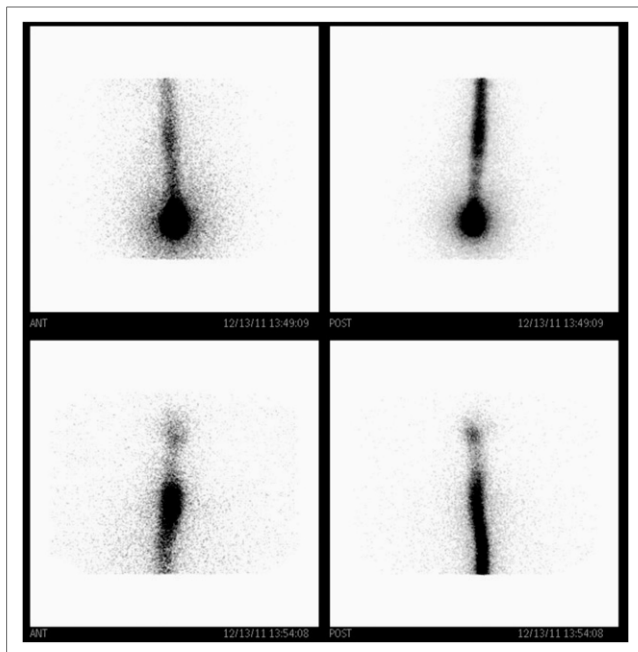


**FIGURE 1.** Planar images 30 min after injection of  $^{111}\text{In}$ -DTPA confirm radiotracer activity in subarachnoid space, with cephalad migration up spinal column.

and 8 subsets, and a Butterworth filter with a 0.5 cutoff and order of 5.0. The CT scan had the following parameters: 5-mm thickness, 120 kV, 50 mAs,  $16 \times 1.5$  collimation, 0.813 pitch, 0.75-s rotation time, 600-mm field of view, and matrix of 512. If planar imaging at 24 h is equivocal, SPECT/CT images can be performed at 48 h.

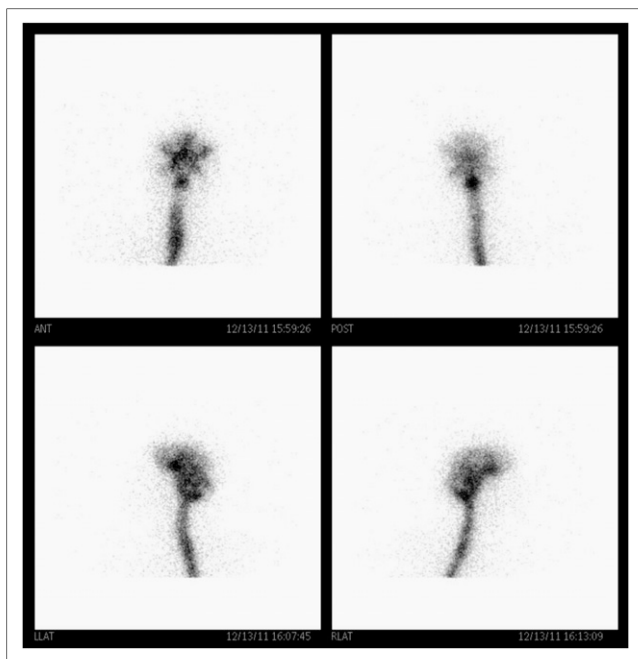


**FIGURE 2.** Anterior, posterior, and lateral planar images 4 h after injection demonstrate reflux of radiotracer into lateral ventricles.

The planar images at 4 h demonstrated reflux into the lateral ventricles (Fig. 2)—a normal finding. However, [Fig. 2] the ventricular reflux persisted at 24 h (Fig. 3). This [Fig. 3] scintigraphic appearance has been described as a heart configuration on the anterior view, butterfly configuration on the posterior view, and a comma or C-shaped configuration on lateral views (8). Additionally, SPECT/CT images at 24 h confirmed localization of radiotracer activity into the lateral ventricles demonstrating the previously mentioned characteristic appearances. No flow over the convexities was demonstrated, as is consistent with NPH (Fig. 4). [Fig. 4]

## DISCUSSION

A variety of imaging modalities can be used to evaluate for NPH. CT and MR imaging are usually the first steps because they can often exclude other causes of the patients' symptoms, but the findings from these modalities are usually nonspecific. Pertinent findings for NPH include dilatation of the ventricles out of proportion to sulcal and basal cistern prominence. MR imaging is usually superior to CT because of higher resolution and ability to visualize other markers of NPH, including 3 specific findings of NPH. These include periventricular white matter lesions, which are thought to represent a transependymal exit of CSF (9,10); aqueduct flow void, or the CSF flow void sign, which represents loss of signal in the aqueduct of Sylvius from high CSF velocity (10,11); and corpus callosum thinning, which may be attributed to either small areas of infarction or atrophy from ventricular dilatation (10). In addition, newer MR imaging techniques such as phase contrast cine-MR imaging and perfusion-weighted MR imaging may be used to evaluate NPH by measuring the pulsatile velocity of CSF during cardiac systole or by evaluating changes in cerebral blood flow, respectively (12,13). MR cisternography, another modern technique, uses intrathecal administration of gadolinium-DTPA for diagnosis of NPH and has higher soft-tissue resolution and better CSF-to-brain contrast than the radionuclide technique (14). Lastly, MR spectroscopy can be used to demonstrate markers of neuronal dysfunction in NPH, such as an increased ratio of *N*-acetyl-aspartate to creatine in the medial frontal cortex (15).

Radionuclide cisternography is a functional imaging tool with documented use as early as the 1950s. This imaging study provides information on CSF circulation. A radiotracer is injected into the intrathecal space, and serial images are taken to study the flow of CSF. The study is invasive and operator-dependent, requiring a lumbar puncture and subarachnoid instillation of the radiotracer. Historically, intrathecal or intraventricular injection of radioiodinated ( $^{131}\text{I}$ ) human serum albumin was used for cisternography (16). However, this radiotracer is no longer used clinically because of reports of symptomatic aseptic chemical meningitis (17), as well as other disadvantages of  $^{131}\text{I}$ , including a long half-life (8 d),  $\beta$  emission (associated

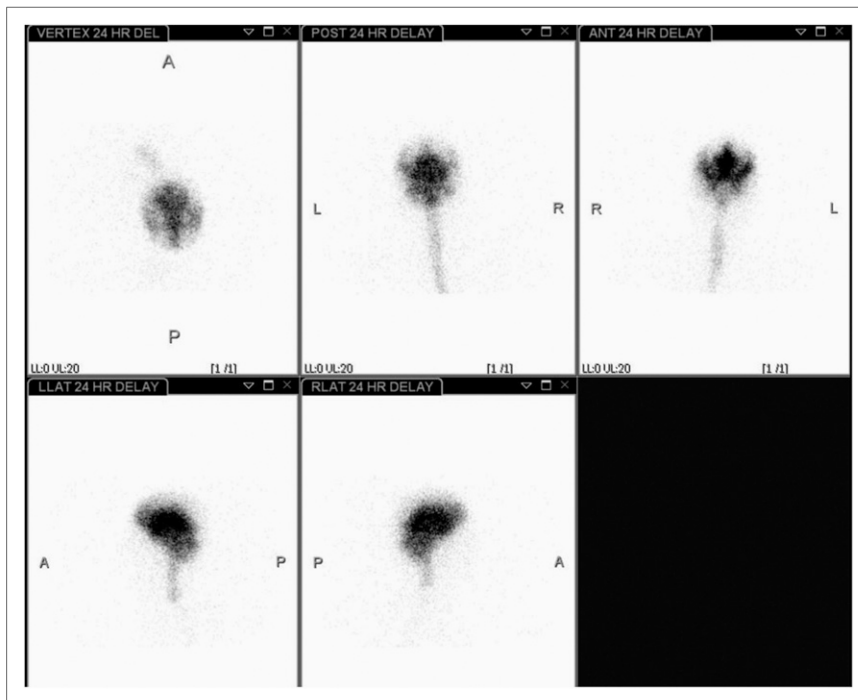


**FIGURE 3.** Planar images 24 h after injection show persistent reflux into ventricles, with no flow over convexities. Shown clockwise from top left are axial, posterior, anterior, right lateral, and left lateral projections of head and neck.

with a relatively high dose to the patient), and rather poor imaging characteristics (18). Other radiotracers, such as  $^{99m}\text{Tc}$ -inulin and chelated  $^{169}\text{Yb}$ , were also used previously but now have been replaced by  $^{111}\text{In}$ -DTPA because of the optimal half-life of  $^{111}\text{In}$  (2.8 d), allowing for delayed imaging, reasonable  $\gamma$ -photon energies, and absence of  $\beta$  radiation. The chelating agent, DTPA, is not lipid-soluble, is not metabolized, and is not absorbed until it reaches the arachnoid villi (6). When injected into the subarachnoid space,  $^{111}\text{In}$ -DTPA can provide physiologic information on CSF dynamics, with minimal radiation dose to the patient and no direct adverse effects.

A variety of CSF flow patterns can be demonstrated on radionuclide cisternography. The classic findings of NPH include abnormal reflux of radiotracer into the ventricles and absence of activity over the convexities on delayed images (3,6,19). Five types of CSF movement patterns have [Fig. 5] been described on cisternograms (Fig. 5) (6). Type I, which

can be either normal or seen in a noncommunicating hydrocephalus, shows radiotracer movement over the convexities at 24 h. In type II, there is delayed migration over the convexities, but no ventricular reflux is noted. This pattern can be seen in cerebral atrophy or in advanced age. The type IIIA pattern demonstrates transient ventricular reflux, with radiotracer activity over the convexities. This pattern is considered to be indeterminate, because it can be seen in either evolving or resolving communicating hydrocephalus. If there is no migration of radiotracer over the convexities at 24 h with transient ventricular activity, the pattern is type IIIB. However, if the ventricular activity persists at 24 h, the pattern is type IV. The last two patterns can support a clinical diagnosis of NPH, and patients with these patterns were once thought to benefit the most after CSF shunting, with a sensitivity of 88% in predicting a good response (20–22). Conversely, more recent studies have indicated that radionuclide cisternography is an unreliable predictor, showing

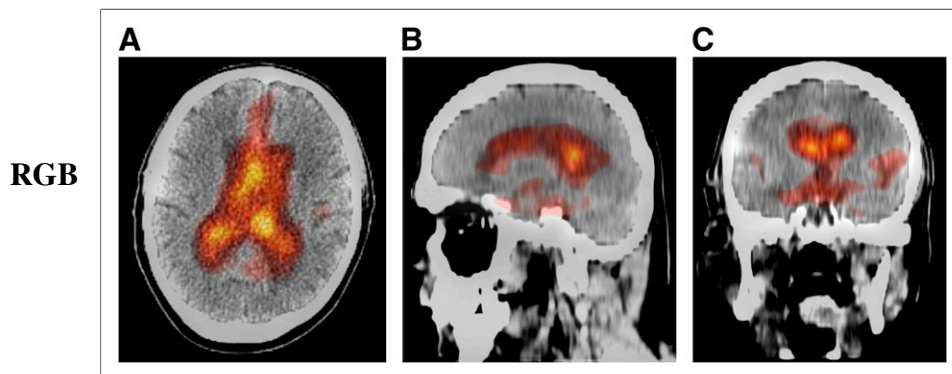
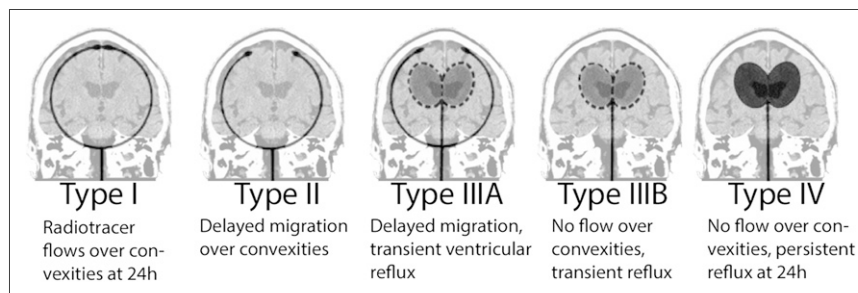


**FIGURE 4.** SPECT/CT images at 24 h using Smart color map (Philips) in axial (A), sagittal (B), and coronal (C) reconstructions demonstrate reflux into lateral ventricles in butterfly, comma, and heart configurations, respectively. Additionally, coronal images demonstrate radiotracer activity localized to Sylvian fissures.

**FIGURE 5.** Cisternographic CSF flow patterns as seen on anterior planar or coronal SPECT projections. (Modified with permission from (6).)



many false-positives and failure to demonstrate response to VP shunting (23–26). A relatively high complication rate of up to 31% has been reported in radionuclide cisternography studies (27). Furthermore, the lack of anatomic details for radionuclide cisternography in comparison with MR imaging has caused the former to fall largely out of favor, especially with introduction of the new MR techniques discussed previously.

Hybrid imaging with SPECT/CT has led to major improvements in diagnostic accuracy by fusing functional studies with anatomic images. The disadvantage of these combined systems is the high radiation dose to the patient. For the radionuclide cisternography study alone using 18.5 MBq (0.5 mCi) of  $^{111}\text{In}$ -DTPA, the effective dose to the CNS has been reported to be 3–10 mSv (5,28). In a CT scan of the head, the patient receives approximately 2 mSv, depending on the scan parameters and technique (0.3–6 mSv) (29). On the basis of these estimations, the combined effective dose for a radionuclide cisternography study with SPECT/CT can range between 3 and 16 mSv. Despite the risks associated with ionizing radiation, hybrid SPECT/CT has many valuable indications, particularly for the evaluation of CSF dynamics, with the benefit of anatomic localization. Novotny et al. described the usefulness of SPECT/CT cisternography in localizing sites of CSF leakage (30). Similarly, this technique can be used for evaluation of NPH. Not only does this technique provide accurate localization of radiotracer activity within the precise anatomic spaces, it also provides information on the presence or absence of other structural abnormalities that can contribute to the patients' symptomatology, such as cerebral infarction, hemorrhage, atrophy, and neoplasm (4). Radionuclide cisternography with SPECT/CT can be a valuable alternative to MR imaging for patients who have claustrophobia or contraindications to MR imaging such as incompatible implants and certain pacemakers.

## CONCLUSION

Although MR imaging is noninvasive, has superior resolution, is not associated with ionizing radiation, and can use multiple different sequences to evaluate CSF dynamics, radionuclide cisternography with SPECT/CT is an alternative imaging modality for those unable to

undergo MR imaging. This technique combines both functional and anatomic imaging to provide precise information on CSF dynamics together with evidence on other structural abnormalities.  $^{111}\text{In}$ -DTPA cisternography with SPECT/CT is a complementary diagnostic tool that, when combined with clinical and laboratory findings, can be a valuable imaging method for evaluation of NPH.

## DISCLOSURE

No potential conflict of interest relevant to this article was reported.

## REFERENCES

- Klassen BT, Ahlskog JE. Normal pressure hydrocephalus: how often does the diagnosis hold water? *Neurology*. 2011;77:1119–1125.
- Krauss JK, Halve B. Normal pressure hydrocephalus: survey on contemporary diagnostic algorithms and therapeutic decision-making in clinical practice. *Acta Neurochir (Wien)*. 2004;146:379–388.
- Mettler FA, Guiberteau MJ. *Essentials of Nuclear Medicine Imaging*. Philadelphia, PA: Saunders/Elsevier; 2006.
- Chuang T-L, Hsu M-C, Wang Y-F. Normal pressure hydrocephalus: scintigraphic findings on SPECT/CT image. *Ann Nucl Med Sci*. 2010;23:169–174.
- Sandler MP, Coleman RE, Patton JA, Wackers FJT, Gottschalk A. *Diagnostic Nuclear Medicine*. Philadelphia, PA: Lippincott Williams & Wilkins; 2003.
- Ziessman HA, O'Malley JP, Thrall JH. *Nuclear Medicine: The Requisites*. St. Louis, MO: Mosby; 2006.
- Strecker E-P, James AE. The evaluation of cerebrospinal fluid flow and absorption: clinical and experimental studies. *Neuroradiology*. 1973;6:200–205.
- James AE Jr, New PF, Heinz ER, Hodges FJ III, Deland FH. A cisternographic classification of hydrocephalus. *AJR*. 1972;115:39–49.
- Tullberg M, Hultin L, Ekholm S, Månsson JE, Fredman P, Wikkelsø C. White matter changes in normal pressure hydrocephalus and Binswanger disease: specificity, predictive value and correlations to axonal degeneration and demyelination. *Acta Neurol Scand*. 2002;105:417–426.
- Jack CR Jr, Mokri B, Laws ER Jr, Houser OW, Baker HL Jr, Petersen RC. MR findings in normal-pressure hydrocephalus: significance and comparison with other forms of dementia. *J Comput Assist Tomogr*. 1987;11:923–931.
- Bradley WG, Whittemore A, Kortman K, et al. Marked cerebrospinal fluid void: indicator of successful shunt in patients with suspected normal-pressure hydrocephalus. *Radiology*. 1991;178:459–466.
- Armonda RA, Citrin CM, Foley KT, Ellenbogen RG. Quantitative cine-mode magnetic resonance imaging of Chiari I malformations: an analysis of cerebrospinal fluid dynamics. *Neurosurgery*. 1994;35:214–223.
- Walter C, Hertel F, Naumann E, Mörsdorf M. Alteration of cerebral perfusion in patients with idiopathic normal pressure hydrocephalus measured by 3D perfusion weighted magnetic resonance imaging. *J Neurol*. 2005;252:1465–1471.
- Algin O, Hakyemez B, Ocakoğlu G, Parlak M. MR cisternography: is it useful in the diagnosis of normal-pressure hydrocephalus and the selection of "good shunt responders"? *Diagn Interv Radiol*. 2011;17:105–111.

15. del Mar Matarín M, Pueyo R, Poca MA, et al. Post-surgical changes in brain metabolism detected by magnetic resonance spectroscopy in normal pressure hydrocephalus: results of a pilot study. *J Neurol Neurosurg Psychiatry*. 2007;78:760–763.
16. Dichiro G, Reames PM, Matthews WB Jr. RISA-ventriculography and RISA-cisternography. *Neurology*. 1964;14:185–191.
17. Messert B, Rieder MJ. RISA cisternography: study of spinal fluid changes associated with intrathecal RISA injection. *Neurology*. 1972;22:789–792.
18. Matin P, Goodwin DA. Cerebrospinal fluid scanning with <sup>111</sup>In. *J Nucl Med*. 1971;12:668–672.
19. Patten DH, Benson DF. Diagnosis of normal-pressure hydrocephalus by RISA cisternography. *J Nucl Med*. 1968;9:457–461.
20. Ghosh D, Ghosh P, Gambhir S, Kohli A. Normal pressure hydrocephalus: role of radionuclide cisternography. *Neurol India*. 1997;45:231.
21. James AA Jr, Deblanc HJ Jr, Deland FH, Mathews ES. Refinements in cerebrospinal fluid diversionary shunt evaluation by cisternography. *AJR*. 1972;115:766–773.
22. McCullough DC, Harbert JC, Di Chiro G, Ommaya AK. Prognostic criteria for cerebrospinal fluid shunting from isotope cisternography in communicating hydrocephalus. *Neurology*. 1970;20:594–598.
23. Halpern SE, Ashburn WL, Alazraki NP. Radionuclide cisternography: prediction of clinical results of neurosurgical shunting in patients with communicating normal pressure hydrocephalus—fact or fantasy. *J Nucl Med*. 1974;15:465–466.
24. Kilic K, Czorny A, Auque J, Berkman Z. Predicting the outcome of shunt surgery in normal pressure hydrocephalus. *J Clin Neurosci*. 2007;14:729–736.
25. Benzel EC, Pelletier AL, Levy PG. Communicating hydrocephalus in adults: prediction of outcome after ventricular shunting procedures. *Neurosurgery*. 1990;26:655.
26. Vanneste J, Augustijn P, Dirven C, Tan W, Goedhart Z. Shunting normal-pressure hydrocephalus: do the benefits outweigh the risks? A multicenter study and literature review. *Neurology*. 1992;42:54–59.
27. Petersen RC, Mokri B, Laws ER Jr. Surgical treatment of idiopathic hydrocephalus in elderly patients. *Neurology*. 1985;35:307–311.
28. Smith T. Internal exposure of patients and staff in diagnostic nuclear medicine procedures. *J Soc Radiol Prot*. 1984;4:45.
29. Smith-Bindman R, Lipson J, Marcus R, et al. Radiation dose associated with common computed tomography examinations and the associated lifetime attributable risk of cancer. *Arch Intern Med*. 2009;169:2078–2086.
30. Novotny C, Pötzi C, Asenbaum S, Peloschek P, Suess E, Hoffmann M. SPECT/CT fusion imaging in radionuclide cisternography for localization of liquor leakage sites. *J Neuroimaging*. 2009;19:227–234.